ASTRONOMY & ASTROPHYSICS
SUPPLEMENT SERIES

Astron. Astrophys. Suppl. Ser. **126,** 373-378 (1997)

Atomic data from the Iron Project

XXVII. Electron impact excitation collision strengths and rate coefficients for Fe IV⋆

H.L. Zhang and A.K. Pradhan

Department of Astronomy, The Ohio State University, Columbus, OH 43210, U.S.A.
e-mail: zhang@payne.mps.ohio-state.edu

Received February 28; accepted March 3, 1997

Abstract. Collision strengths and maxwellian-averaged rate coefficients have been calculated for 8771 non-vanishing transitions among 140 fine structure levels, dominated by the configurations $3d^5$, $3d^4 4s$, and $3d^4 4p$ in Fe IV. Collision strengths are calculated using the *R*-matrix method with a 49 term close-coupling target expansion for electron energies up to 15 rydbergs. Rate coefficients are tabulated for a wide range of temperatures in which Fe IV is abundant in plasma sources. A brief discussion of the calculations and sample results are given. The present rates for Fe IV are expected to find applications in spectral diagnostics of a variety of astrophysical sources.

Key words: atomic processes — planetary nebulae: general — H II regions

1. Introduction

Fe IV emission lines are observed in stellar sources, such as hot stars and white dwarfs, (Penston et al. 1983 and Holberg et al. 1994; Vennes et al. 1995). Becker & Butler (1995) have modeled non-LTE line formation for Fe IV and synthesized the predominantly UV spectra from hot subdwarfs. According to photoionization models Fe IV is expected to be a dominant ionization stage of iron in nebulae (e.g. Baldwin et al. 1991 and Rubin et al. 1991). However, the Fe IV spectra from H II regions remained elusive until the recent HST observations of the Orion nebula by Rubin et al. (1997), who reported the first detection of Fe IV in the UV [Fe IV] lines at 2836.56 Å arising from the transition $3d^5\ {}^4P_{5/2} \rightarrow 3d^5\ {}^6S_{5/2}$, and the blend of $\lambda\lambda 2568.4, 2568.2$ Å due to $3d^5\ {}^4D_{5/2,3/2} \rightarrow 3d^5\ {}^6S_{5/2}$. From the [Fe IV] lines and the predicted fluxes from photoionization models, they derive an iron depletion in Orion, relative to solar, of up to factors of $70 - 200$. This appears to be excessive; Rubin et al. (1997) suggest the need for improved modeling and a reexamination of the atomic data, especially the electron impact excitation collision strengths used in the analysis.

The only earlier published work on electron impact excitation collision strengths of Fe IV is by Berrington & Pelan (1995) in Paper XII of this series on the Vanadium-like ions. They included the five lowest sextet and quartet *LS* terms $3d^5$ (^{6}S, ^{4}G, ^{4}P, ^{4}D, ^{4}F) in a non-relativistic (NR) calculation, and used algebraic recoupling to obtain excitation rate coefficients for transitions between the 12 fine structure levels of the first four terms.

In our earlier study on Fe III (Zhang & Pradhan 1995a) using the NR and Breit-Pauli (BP) close-coupling R-matrix methods, we concluded that the relativistic effects are small for the forbidden transitions between the low-lying levels, and that the resonances and the coupling effects arising from a large coupled-channel wavefunction expansion dominate the collision strengths. Therefore, as described in Zhang (1996, Paper XVIII), we carried out an 83CC NR calculations for Fe III, neglecting the relativistic intermediate coupling effects. Fine-structure collision strengths were then obtained from the LS coupling data by algebraic recoupling using the code STGFJ.

Similarly, for Fe IV we expect the relativistic effects to be small, especially for the forbidden transitions from the ground level to the low-lying even parity levels since there is no fine-structure splitting for the ground term $3d^5\ {}^6S$. Before carrying out a large-scale calculation, we made test calculations with the BP R-matrix method (Berrington et al. 1995) using a 16-level target expansion (corresponding to the above five terms) and obtained results

Send offprint requests to: H.L. Zhang

⋆ Table 3 for complete data for Fe IV is only available in electronic form at the CDS via anonymous to ftp to cdsarc.u-strasbg.fr (130.79.128.5) or via http://cdsweb.u-strasbg.fr/Abstract.html

similar to those in Paper XII by Berrington & Pelan (1996). These BP calculations, albeit with a small target expansion, showed that the relativistic effects are indeed not important for Fe IV, and also provided the basis for the present calculations, which are much more extensive than those reported earlier in the IP series. Therefore, we have carried out the calculation for Fe IV with a 49-term target expansion (49 CC) using the NR R-matrix method in the close-coupling approximation. Again, the algebraic recoupling method was used to obtain results for a large number of fine-structure transitions. The maxwellian-averaged rate coefficients or effective collision strengths are calculated and tabulated over the temperature range in which Fe IV is most abundant in astrophysical sources. A brief description of the computations and the results are given in the following sections.

The present work is part of an international collaboration known as the IRON Project (Hummer et al. 1993, referred to as Paper I) to obtain accurate electron-impact excitation rates for fine-structure transitions in atomic ions. A full list of the papers in this Atomic Data from the IRON Project series published to-date is given in the references. A complete list of papers including those in press can be found at http://www.am.qub.uk/projects/iron/papers/, where abstracts are also given for each paper. Information on other works by the present authors and their collaborators, including photoionization and recombination of ions of iron and other elements, can be found at http://www-astronomy.mps.ohio-state.edu/∼pradhan/.

2. Atomic calculations

The target expansion for the present calculations, used earlier in Paper XVII (Nahar & Pradhan 1996) for the radiative work for Fe III, consists of 49 LS-terms dominated by the configurations $3d^5$, $3d^4 4s$ and $3d^4 4p$. The 140 fine structure levels of these 49 terms, and their observed energies (Sugar & Corliss 1985), are listed in Table 1. This table also provides the key to the level indices used to identify the transitions in tabulating the maxwellian-averaged collision strengths.

In the present work, as in our earlier Papers III, VI and XVIII, the reactance matrix (the K-matrix) is first calculated and used to evaluate the collision strengths. In the NR algebraic recoupling approach, the K-matrices are obtained as usual by the different stages of the R-matrix package (Berrington et al. 1995) in LS coupling. The K-matrices are subsequently transformed from LS coupling to pair coupling (Eissner et al. 1974), using the STGFJ code (Luo & Pradhan 1990; Zhang & Pradhan 1995a), which is an extension of the asymptotic region code, STGF, of the R-matrix codes (Hummer et al. 1993). The collision strengths were calculated for a large number of electron energies ranging from 0 to 15 rydbergs. The energy range is carefully chosen in order to obtain detailed collision strengths in the region where they are dominated by resonances, as well as in an extended region where resonances are not important or have not been included, but which are necessary to obtain accurate maxwellian-averaged rate coefficients, particularly for dipole allowed transitions.

In order to delineate the resonance structures, an effective quantum number mesh (ν-mesh) was used to obtain the collision strengths at 5604 energy points in the range $E = 0 - 1.789$ rydbergs. The ν-mesh ensures equal sampling of resonances in each interval $(\nu, \nu + 1)$, where $\nu(E) = z/\sqrt{(E - E_{\rm t})}$ and $E_{\rm t}$ is the energy of the particular target threshold to which the resonance series converges. In the energy region $E > 1.789$ rydbergs, the collision strengths were calculated for 20 additional energies up to 15 rydbergs. It is impractical to carry through the calculation of collision strengths at an even larger number of energies, as the number of scattering channels increases across higher target thresholds. The calculations are therefore optimised to obtain extensive delineation of resonances for the collision strengths for forbidden transitions in the low energy region that contributes predominantly to the maxwellian rate coefficient. For the optically allowed transitions, the dominant contribution arises from higher partial waves and in higher energy regions since $\Omega \sim \ln(\epsilon)$; here, however, resonances are relatively less important.

We include partial wave contributions from total angular momenta of the electron plus target system $J = 0 - 11$ (where $J = L + S$; L and S are total orbital and spin angular momenta). The corresponding SL's, for both even and odd parities, are

$0 \le L \le 11,\ (2S+1) = 1$
$0 \le L \le 12,\ (2S+1) = 3$
$0 \le L \le 13,\ (2S+1) = 5$
$0 \le L \le 14,\ (2S+1) = 7.$

These should be sufficient to ensure convergence for the non-optically allowed transitions. As in the Fe II (Paper III) and Fe III (Paper XVIII) work, the Coulomb-Bethe approximation was employed to account for the large ℓ contributions to the collision strengths for optically allowed transitions at energies greater than 1.789 rydbergs. The electric dipole line strengths required for the Coulomb-Bethe approximation were derived from the Opacity Project database TOPbase (Cunto et al. 1992). The oscillator strengths in the TOPbase were transformed to line strengths in LS coupling and then algebraically recoupled to obtain fine structure values using a code by Sultana Nahar.

3. Results

We present a small sample of the collision strengths and compare the maxwellian-averaged collision strengths from the present 49-term calculation with those from the

Table 1. The 140 fine structure levels corresponding to the 49 *LS* terms included in the calculations and their observed energies (Ry) in Fe IV (Sugar & Corliss 1985)

i	Term		J	Energy	i	Term		J	Energy
1	$3d^5$	^6S	5/2	0.00000	54	$3d^4(^3F2)4s$	^4F	9/2	1.42360
2	$3d^5$	^4G	11/2	0.29384	55			7/2	1.42270
3			9/2	0.29427	56			5/2	1.42200
4			7/2	0.29439	57			3/2	1.42170
5			5/2	0.29435	58	$3d^4(^3G)4s$	^4G	11/2	1.45200
6	$3d^5$	^4P	5/2	0.32126	59			9/2	1.45100
7			3/2	0.32198	60			7/2	1.44900
8			1/2	0.32265	61			5/2	1.44650
9	$3d^5$	^4D	7/2	0.35338	62	$3d^4(^3P2)4s$	^2P	3/2	1.47230
10			5/2	0.35480	63			1/2	1.45820
11			3/2	0.35483	64	$3d^4(^3H)4s$	^2H	11/2	1.46510
12			1/2	0.35445	65			9/2	1.46090
13	$3d^5$	^2I	13/2	0.42912	66	$3d^4(^3F2)4s$	^2F	7/2	1.47710
14			11/2	0.42901	67			5/2	1.47690
15	$3d^5$	^2D	5/2	0.45146	68	$3d^4(^3G)4s$	^2G	9/2	1.50720
16			3/2	0.45610	69			7/2	1.50310
17	$3d^5$	^2F	7/2	0.46834	70	$3d^4(^3D)4s$	^4D	7/2	1.50810
18			5/2	0.47538	71			5/2	1.50910
19	$3d^5$	^4F	9/2	0.47952	72			3/2	1.51020
20			7/2	0.48020	73			1/2	1.51090
21			5/2	0.48150	74	$3d^4(^1G2)4s$	^2G	9/2	1.52830
22			3/2	0.48149	75			7/2	1.52910
23	$3d^5$	^2H	11/2	0.51367	76	$3d^4(^1I)4s$	^2I	13/2	1.53570
24			9/2	0.51084	77			11/2	1.53610
25	$3d^5$	^2G	9/2	0.52599	78	$3d^4(^1S2)4s$	^2S	1/2	1.55580
26			7/2	0.52314	79	$3d^4(^3D)4s$	^2D	5/2	1.56140
27	$3d^5$	^2F	7/2	0.55819	80			3/2	1.56260
28			5/2	0.55730	81	$3d^4(^1D2)4s$	^2D	5/2	1.61300
29	$3d^5$	^2S	1/2	0.60800	82			3/2	1.61360
30	$3d^5$	^2D	5/2	0.67555	83	$3d^4(^1F)4s$	^2F	7/2	1.66910
31			3/2	0.67522	84			5/2	1.66910
32	$3d^5$	^2G	9/2	0.75539	85	$3d^4(^5D)4p$	$^6F^o$	11/2	1.73390
33			7/2	0.75542	86			9/2	1.72700
34	$3d^5$	^2P	3/2	0.91234	87			7/2	1.72140
35			1/2	0.91242	88			5/2	1.71710
36	$3d^5$	^2D	5/2	0.98637	89			3/2	1.71400
37			3/2	0.98652	90			1/2	1.71210
38	$3d^4(^5D)4s$	^6D	9/2	1.17520	91	$3d^4(^5D)4p$	$^6P^o$	7/2	1.73350
39			7/2	1.17140	92			5/2	1.73150
40			5/2	1.16820	93			3/2	1.73040
41			3/2	1.16580	94	$3d^4(^3P1)4s$	^4P	5/2	1.73120
42			1/2	1.16430	95			3/2	1.73880
43	$3d^4(^5D)4s$	^4D	7/2	1.26520	96			1/2	1.74360
44			5/2	1.26060	97	$3d^4(^3F1)4s$	^4F	9/2	1.73430
45			3/2	1.25710	98			7/2	1.73530
46			1/2	1.25480	99			5/2	1.73540
47	$3d^4(^3P2)4s$	^4P	5/2	1.41930	100			3/2	1.73510
48			3/2	1.40770	101	$3d^4(^5D)4p$	$^4P^o$	5/2	1.76380
49			1/2	1.40020	102			3/2	1.74680
50	$3d^4(^3H)4s$	^4H	13/2	1.41000	103			1/2	1.74070
51			11/2	1.40800					
52			9/2	1.40630					
53			7/2	1.40500					

16-level BP calculation and those by Berrington & Pelan (Paper XII); all non-vanishing maxwellian-averaged collision strengths are given in Table 3, located in a computer file available on request.

Figure 1 shows a comparison of the collision strengths for the transitions from the ground level $3d^5\ ^6S_{3/2}$ to $3d^5\ ^4G_{11/2}$, $3d^5\ ^4P_{5/2}$ and $3d^5\ ^4D_{7/2}$ from the 49CC NR calculations (left) and from the 16-level BP calculation (right). The panels on the right are on smaller energy scales to reveal the detailed resonance structures obtained with a finer energy mesh in the BP calculation. It should be mentioned that similar detailed resonance structures would also be obtained for the 49CC case as for the BP case if a finer energy mesh had been used for the energy range 0 to 0.5 Ryd. However, this does not significantly affect the rate coefficients, except for a slight loss of

Table 1. continued

i	Term		J	Energy	i	Term		J	Energy
104	$3d^4(^5D)4p$	$^6D^o$	9/2	1.76590	123	$3d^4(^3H)4p$	$^4H^o$	13/2	1.94250
105			7/2	1.76230	124			11/2	1.93840
106			5/2	1.75510	125			9/2	1.93530
107			3/2	1.76120	126			7/2	1.93310
108			1/2	1.75980	127	$3d^4(^3P2)4p$	$^4D^o$	7/2	1.96120
109	$3d^4(^3P1)4s$	^2P	3/2	1.78480	128			5/2	1.95300
110			1/2	1.79410	129			3/2	1.94510
111	$3d^4(^3F1)4s$	^2F	7/2	1.78730	130			1/2	1.93930
112			5/2	1.78810	131	$3d^4(^3F2)4p$	$^4G^o$	11/2	1.96840
113	$3d^4(^5D)4p$	$^4F^o$	9/2	1.79380	132			9/2	1.96270
114			7/2	1.79110	133			7/2	1.95950
115			5/2	1.78910	134			5/2	1.95760
116			3/2	1.78780	135	$3d^4(^3H)4p$	$^4I^o$	15/2	1.97630
117	$3d^4(^1G1)4s$	^2G	9/2	1.83330	136			13/2	1.97170
118			7/2	1.83360	137			11/2	1.96660
119	$3d^4(^5D)4p$	$^4D^o$	7/2	1.84630	138			9/2	1.96060
120			5/2	1.84380	139	$3d^4(^3H)4p$	$^2G^o$	9/2	1.97220
121			3/2	1.84150	140			7/2	1.96940
122			1/2	1.84000					

Table 2. Comparison of the effective collision strengths Υ from the 49-term non-relativistic calculation (49CC), from 16-level relativistic Breit Pauli (BP) calculation, and from Berrington & Pelan (1995, Paper XII). i and j, referred to Table 1, are the initial level and the final levels

		$\log T = 3.6$			$\log T = 4.6$		
i	j	49CC	BP	Paper XII	49CC	BP	Paper XII
1	2	1.38e+00	1.15e+00	1.07e+00	1.00e+00	8.82e−01	8.27e−01
1	3	1.15e+00	9.98e−01	8.94e−01	8.37e−01	7.44e−01	6.89e−01
1	4	9.21e−01	7.99e−01	7.16e−01	6.70e−01	6.00e−01	5.51e−01
1	5	6.91e−01	5.98e−01	5.37e−01	5.02e−01	4.55e−01	4.13e−01
1	6	5.91e−01	4.91e−01	4.55e−01	4.83e−01	4.06e−01	3.85e−01
1	7	3.94e−01	3.36e−01	3.03e−01	3.22e−01	2.73e−01	2.57e−01
1	8	1.97e−01	1.60e−01	1.52e−01	1.61e−01	1.34e−01	1.28e−01
1	9	5.47e−01	5.56e−01	5.20e−01	5.88e−01	5.24e−01	5.00e−01
1	10	4.10e−01	4.15e−01	3.90e−01	4.41e−01	3.99e−01	3.75e−01
1	11	2.74e−01	2.85e−01	2.60e−01	2.94e−01	2.70e−01	2.50e−01
1	12	1.37e−01	1.39e−01	1.30e−01	1.47e−01	1.33e−01	1.25e−01
2	3	3.45e+00	2.67e+00	3.89e+00	2.26e+00	1.89e+00	2.68e+00
2	4	7.76e−01	6.01e−01	5.08e−01	4.56e−01	2.99e−01	3.20e−01
2	5	1.63e−01	1.50e−01	5.36e−02	9.30e−02	5.81e−02	3.18e−02
2	6	7.27e−01	6.32e−01	8.10e−01	6.16e−01	4.78e−01	4.74e−01
2	7	3.64e−01	3.15e−01	4.81e−01	3.00e−01	2.40e−01	2.58e−01
2	8	4.00e−02	2.29e−02	2.75e−02	3.32e−02	1.10e−02	9.92e−03
2	9	1.88e+00	1.46e+00	1.28e+00	1.48e+00	1.25e+00	1.10e+00
2	10	7.64e−01	6.29e−01	6.00e−01	6.67e−01	5.53e−01	5.05e−01
2	11	2.61e−01	2.62e−01	2.38e−01	2.44e−01	2.33e−01	2.12e−01
2	12	6.38e−02	6.28e−02	5.88e−02	5.86e−02	5.77e−02	5.34e−02
6	7	8.70e−01	6.36e−01	6.50e−01	7.06e−01	5.27e−01	4.96e−01
6	8	3.06e−01	1.91e−01	2.20e−01	2.44e−01	1.41e−01	1.40e−01
6	9	8.85e−01	6.82e−01	6.56e−01	8.06e−01	6.15e−01	6.00e−01
6	10	5.57e−01	3.92e−01	4.33e−01	5.11e−01	3.41e−01	3.47e−01
6	11	2.99e−01	2.16e−01	2.34e−01	2.68e−01	1.87e−01	1.76e−01
6	12	1.24e−01	8.52e−02	9.58e−02	1.07e−01	7.37e−02	6.69e−02
9	10	1.25e+00	8.16e−01	8.62e−01	9.74e−01	7.24e−01	6.93e−01
9	11	4.47e−01	2.10e−01	2.14e−01	3.34e−01	1.65e−01	1.52e−01
9	12	1.88e−01	8.47e−02	8.67e−02	1.42e−01	6.72e−02	6.19e−02

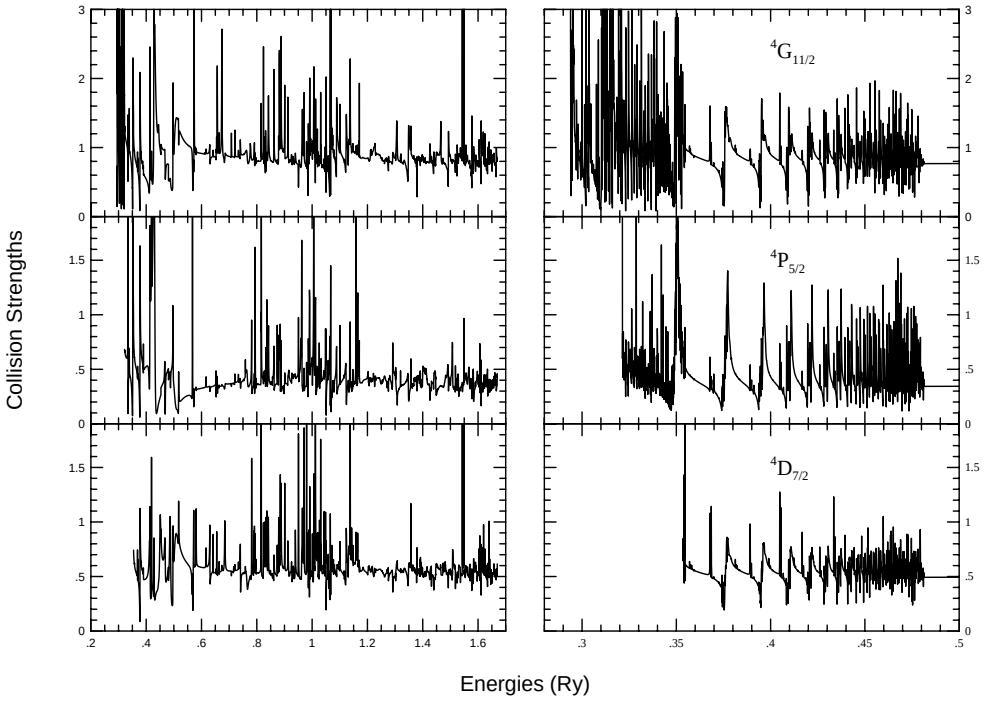

Fig. 1. The collision strengths for the forbidden transitions from the ground level $3d^5\ ^6S_{3/2}$ to $3d^5\ ^4G_{11/2}$, $3d^5\ ^4P_{5/2}$ and $3d^5\ ^4D_{7/2}$ from the 49CC NR calculations (left panels) and from the 16-level BP calculation (right panels). Note the different energy scales in the right and the left panels

accuracy at very low temperatures. It is seen from Fig. 1 that owing to the larger target expansion the resonance structures in the 49CC NR case are more extensive than in the 16-level BP case. Consequently, as seen below, the 49CC rate coefficients show a much larger resonance enhancement.

Figure 2 shows the collision strengths for the optically allowed transitions $3d^5\ ^6S_{5/2} - 3d^4 4p\ ^6P^o_{7/2}$, $3d^5\ ^4G_{11/2} - 3d^4 4p\ ^4F^o_{9/2}$ and $3d^5\ ^4P_{5/2} - 3d^4 4p\ ^4P^o_{5/2}$. As mentioned earlier, the Coulomb-Bethe approximation was employed to estimate the contributions by higher partial waves. It is clear from this figure that relative resonance contributions are not as strong as in the forbidden transitions and that the rate coefficients are dominated by the high energy region where the collision strength has the Bethe asymptotic behavior, $\Omega \sim \ln(\epsilon)$.

The procedure for obtaining maxwellian-averaged collision strengths or effective collision strengths can be found in earlier publications in this series (e.g. see Papers I, VI or XVIII). In Table 2 we compare the present results (49CC) for some transitions at two temperatures, 3981 K and 39811 K, with those from our 16-level BP calculation (BP) and from Berrington & Pelan (1995, Paper XII). In this table, the BP results are quite close to those in Paper XII, indicating that the relativistic effects are not important for these transitions, while the 49CC results are generally larger than the above two entries, indicating large enhancements due to resonance and coupling effects.

The maxwellian-averaged collision strengths were calculated for all 8771 non-vanishing transitions between the 140 energy levels shown in Table 1, for 20 temperatures ranging from 2000 to 500000 K. The entire dataset of effective collision strengths in the above temperature range is tabulated in Table 3. It is noted that collision strengths for some of the transitions vanish due to a restriction on the quantum numbers of the initial and final levels, such as, for example, the large spin-change transitions between sextets and doublets. These are not included in Table 3. Table 3 is available only in electronic form from the CDS or via ftp from the authors at: zhang@payne.mps.ohio-state.edu.

4. Discussion and conclusion

In this section we estimate the accuracy of our results.

The fine $\nu-$mesh below $E = 1.789$ Ry, for excitation to the lower-lying, even-parity levels, fully resolves the important resonance features associated with the sextet and quartet odd-parity levels up to the $^4F^\circ_J$ levels. Therefore, rate coefficients for this type of transitions should be highly accurate, $\approx 10 - 20\%$. For optically allowed transitions from the low-lying levels to the sextet and quartet odd parity levels with energies below 1.789 Ry, the

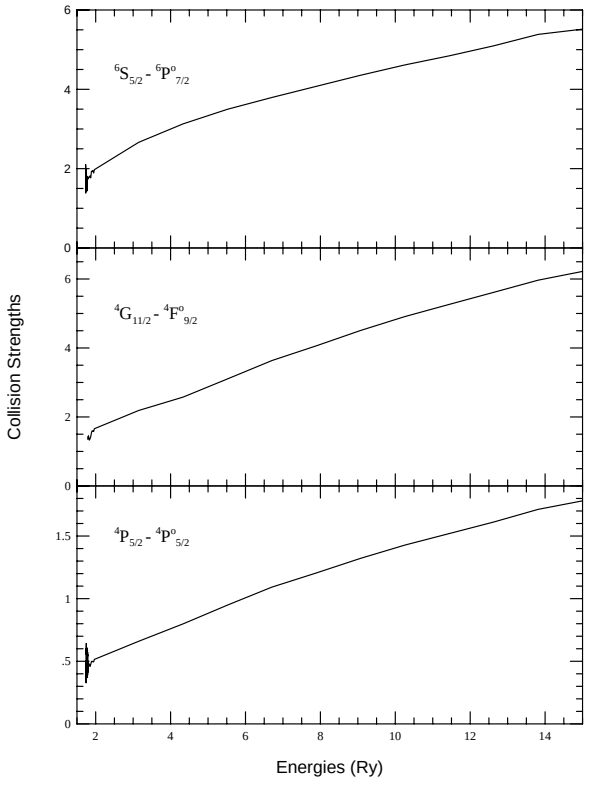

Fig. 2. The collision strengths for the optically allowed transitions **a)** $3d^5\ ^6S_{5/2} - 3d^4 4p\ ^6P^o_{7/2}$, **b)** $3d^5\ ^4G_{11/2} - 3d^4 4p\ ^4F^o_{9/2}$ and **c**) $3d^5\ ^4P_{5/2} - 3d^4 4p\ ^4P^o_{5/2}$ from the 49CC calculation

rate coefficients should also be of the same accuracy since resonances are relatively less important and the collision strengths are large and dominated by the higher partial waves, as seen from Fig. 2. For the forbidden (and intercombination) transitions from the low-lying levels to intermediate energy levels, up to the $^4F^\circ_J$ levels, and transitions between these intermediate-energy levels, the accuracy of the rate coefficients is expected to be less, $\approx 30 - 50\%$. For transitions corresponding to the high-lying levels with threshold energies greater than 1.789 Ry, the uncertainty could exceed 50% since a coarse energy mesh was used and the resonances and coupling effects due to higher terms were neglected. We would also emphasize here that for all transitions the maxwellian-averaged collision strengths for high temperatures (roughly larger than the highest threshold energy included in the target expansion, about 300 000 K in the present case) could have a larger uncertainty, since resonances due to higher target states are not included. However, data for these temperatures are of little astrophysical interest. These general criteria should apply to all our earlier publications in this series.

We hope the present work will provide a reasonably complete collisional dataset for extensive astrophysical diagnostics using Fe IV spectra from various sources.

Acknowledgements. We wish to thank Manuel Bautista for his contribution in obtaining the target wavefunctions and Dr. David Hummer, the coordinator of the IRON Project, for his comments. This work was supported by a grant (PHY-9421898) from the U.S. National Science Foundation. We are also grateful to the Ohio Supercomputer Center in Columbus, Ohio, for their support. Some of the computational work was carried out on the Cray Y-MP8/64, and the asymptotic code, STGFJ, was entirely run on the massively parallel Cray T3D at this center.

References

Baldwin J.A., Ferland G.J., Martin P.G., et al., 1991, ApJ 374, 580
Bautista M.A., Pradhan A.K., 1996, A&AS 115, 551 (Paper XIII)
Bautista M.A., 1996, A&AS 119, 105 (Paper XVI)
Becker S.R., Butler K., 1995, A&A 301, 187
Berrington K.A., 1995, A&AS 109, 193 (Paper VIII)
Berrington K.A., Eissner W.B., Norrington P.H., 1995, Comp. Phys. Comm. 92, 290
Berrington K.A., Pelan J.C., 1995, A&AS 114, 367 (Paper XII); 1996, Erratum (in press)
Berrington K.A., Zeippen C.J., Le Dourneuf M., Eissner W., Burk P.G., 1991, J. Phys. B 24, 3467
Butler K., Zeippen C.J., 1994, A&AS 108, 1 (Paper V)
Cunto W., Mendoza C., 1992, Rev. Mexicana Astron. Astrofis. 23, 107
Eissner W., Jones M., Nussbaumer H., 1974, Comput. Phys. Commun 8, 270
Holberg J.B., Hubeny I., Barstow M.A., Lanz T., Sion E.M., Tweedy R.W., 1994, ApJ 425, L105
Hummer D.G., Berrington K.A., Eissner W., et al., 1993, A&A 279, 298 (Paper I)
Kisielius R., Berrington K.A., Norrington P.H., 1996, A&AS 118, 157 (Paper XV)
Lennon D.J., Burke V.M., 1994, A&AS 103, 273 (Paper II)
Luo D., Pradhan A.K., 1990, Phys. Rev. A 41, 165
Nahar S.N., 1995, A&A 293, 967 (Paper VII)
Nahar S.N., Pradhan A.K., 1996, A&AS 119, 509 (Paper XVII)
Pelan J., Berrington K.A., 1995, A&AS 110, 209 (Paper IX)
Penston M.V., Benvenuti P., Cassatella A., et al., 1983, MNRAS 202, 833
Rubin R.H., Dufour R.J., Ferland G.J., et al., 1997 ApJ 474, L131
Rubin R.H., Simpson J.P., Haas M.R., Erickson E.F., 1991, ApJ 374, 564
Saraph H.E., Storey P.J., 1996, A&AS 115, 151 (Paper XI)
Saraph H.E., Tully J.A., 1994, A&AS 107, 29 (Paper IV)
Storey P.J., Mason H.E., Saraph H.E., 1996, A&A 309, 677 (Paper XIV)
Sugar J., Corliss C., 1985, J. Phys. Chem. Ref. Data 14, Suppl. 2
Vennes S., 1995, in Astrophysics in the Extrema Ultraviolet, IAU Symposium No. 152, Bower S. (ed.). Kluwer Academic Publishers, Netherland, p. 193
Zhang H.L., Graziani M., Pradhan A.K., 1994, A&A 283, 319 (Paper III)
Zhang H.L. Pradhan A.K., 1995a, J. Phys. B 28, 3403
Zhang H.L. Pradhan A.K., 1995b, A&A 293, 953 (Paper VI)
Zhang H.L. 1996, A&AS 119, 523 (Paper XVIII)